Studies of Magnetic Shielding for Phototubes ⋆

S. Denisov [a], J. Dickey [b], A. Dzierba [b,*], W. Gohn [b], R. Heinz [b], D. Howell [b], M. Mikels [b], D. O'Neill [b], V. Samoylenko [a], E. Scott [b], P. Smith [b], S. Teige [b]

[a] *Institute for High Energy Physics, Protvino, Moscow Region, 142281 Russia*

[b] *Department of Physics, Indiana University, Bloomington, IN 47405 USA*

Abstract

Phototubes associated with a Cerenkov counter, with a wall of scintillation counters for time-of-flight measurements and with a wall of lead glass blocks of an electromagnetic calorimeter will operate in the fringe field of a superconducting solenoid in the GlueX experiment. The solenoid will be operated with a central magnetic field of ≈ 2.5 T. The maximum fringe field in the vicinity of the phototubes will be approximately 150 G. Various techniques for magnetic shielding of phototubes were studied using a 1-m diameter Helmholtz coil arrangement operated with a maximum central field of 200 G. Results are presented.

Key words: magnetic shielding, phototubes, helmhlotz coils
PACS: 41.20.Gz, 29.30.Aj

⋆ This paper reports on research carried out on behalf of the GlueX/Hall D collaboration at Jefferson Lab in Newport News, VA USA

* Corresponding author.
Email address: dzierba@indiana.edu (A. Dzierba).

1 Introduction

1.1 The GlueX experiment

The goal of the GlueX/Hall D [1] project at Jefferson Lab (JLab) is to map the spectrum of gluonic excitations starting with exotic hybrid mesons – mesons with J^{PC} quantum numbers that are not possible for a simple $q\bar{q}$ bound state. Knowledge of the spectrum of gluonic excitations is necessary for a quantitative understanding of confinement in quantum chromodynamics. Although some tantalizing hints of exotic mesons exist, extensive searches with π and K have not yielded solid evidence of exotic hybrids. Photons are expected to be particularly effective at producing exotic mesons.

The GlueX detector, shown in Figure 1, will use a beam of 9 GeV linearly polarized photons produced via coherent bremsstrahlung from 12 GeV electrons passing through a thin diamond wafer. The GlueX detector will employ a superconducting solenoid magnet to contain the electromagnetic background produced by the intense photon beam (up to 10^8 tagged photons/s) passing through a 30 cm liquid hydrogen target and to analyze the momentum of charged particles. The GlueX detector design is optimized to carry out a full amplitude analysis of final states. This requires excellent hermeticity, resolution and particle identification. Downstream of the solenoid are a Cerenkov counter and a wall of scintillation counters for time-of-flight (TOF) [2] determination. Those are followed by an electromagnetic detector (FCAL) [3,4] consisting of 2500 blocks of lead glass.

The GlueX detector will be housed in a new experimental hall, Hall D, at JLab. GlueX and Hall D are part of the 12 GeV upgrade at Jefferson Lab that will include an energy upgrade of the Continuous Beam Accelerator Facility (*CEBAF*) at JLab from 6 GeV to 12 GeV.

1.2 Magnetic shielding requirements

The phototubes associated with the Cerenkov counter, TOF and FCAL will be located in the fringe field of the solenoid. The central field of the solenoid will be 2.5 T. Magnetic field simulations indicate a maximum fringe field of approximately 150 G in the vicinity of the Cerenkov, TOF and FCAL phototubes.

The Cerenkov counter will be a threshold counter using C_4F_{10} at 1 atm with phototubes that will have photocathodes at least 5 inch diameter. Magnetic shielding will be required to reduce the field at these phototubes to less than

0.5 G. The TOF phototubes will be Philips XP2020. The phototubes will exist outside the TOF wall and can be oriented either horizontally (along the axis of the solenoid) or vertically.

The lead glass electromagnetic calorimeter, FCAL, to be used in the GlueX experiment will be a modification of the 3053-element lead glass calorimeter used in experiment E852 at Brookhaven lab and described in references [3,4]. In that experiment the calorimeter was located downstream of the Brookhaven MPS spectrometer dipole magnet with a central field of about 2 T. The phototubes associated with the lead glass calorimeter were FEU-84-3 made in Russia. They have a 3.4 cm outer diameter and a length of 10 cm. The phototubes were registered against the stack of lead glass blocks using a cellular wall. The blocks had a cross section of 4×4 cm^2. The cellular wall consisted of two aluminum plates with soft iron shields that were press fit into holes in the plates. The holes were on 4 cm centers with a diameter slightly less than 4 cm. The phototubes were wrapped in μ-metal 300 μm thick. For the GlueX experiment, the lead glass block stack will be roughly circular rather than rectangular. The 5 meter distance from the magnet center to phototube wall will be about the same as in E852. The fringe field will be that of a solenoid rather than the dipole of E852. From the E852 experience, the FEU-84-3 can operate in magnetic fields up to 5 G.

1.3 Outline

This paper describes magnetic shielding studies using a Helmholtz coil arrangement producing a maximum central field of 200 G. Section 2 describes the construction of the Helmholtz coils and initial mapping of the magnetic field and comparison of measurements with field simulations. Information on coil heating is also presented. Section 3 deals with the measurement of the magnetic field inside iron tubes of various dimensions, with and without μ-metal. Measurements were carried out with shields aligned along and transverse to the axial field of the Helmholtz coils. Measurements included measuring the magnetic field inside shields and by studying the effect of shielding on the count rate of phototubes with radioactive sources. Section 4 summarizes our conclusions.

2 Helmholtz coils

2.1 Construction

It is well known that a very uniform magnetic field over a reasonably large region of space can be achieved with Helmholtz coils - a pair of parallel circular coils whose separation is equal to the coil radius. The magnetic field of such an arrangement is within 95% of the central field along the central axis of the two coils from one coil to another. The central magnetic field, as a function of coil radius R, is given by:

$$B(R) = \frac{8\mu_0 NI}{5^{3/2}R} = 0.008992\frac{NI}{R} \tag{1}$$

where B is in G, with R in meters and NI in ampere·turns. In order to have an adequate volume for these tests we chose a radius of 0.5 m.

Initially the Helmholtz coils were designed to produce a central field of 90 G, corresponding to 12,356 A·turns. Each of the two coils was wound with seven separate windings of 10-gauge (2.591 mm diameter) copper wire onto a wooden spool. The resistance of 10-gauge copper wire is 3.28 Ω/km. The total length of wire per coil is 1066 m. The 340 turns of wire in a coil resulted in an approximate square cross section winding 7.5 cm on a side. The seven windings from each coil were connected in parallel to separate Xantrex XDC 20-600 1200 W supplies. Figure 2 shows a plot of the central B-field as a function of total power supply current. The linear fit yields a dependence of magnetic field B on current I given by $B = 0.30 + 0.83 \cdot I$ where B is measured in G and I in amperes. The field at zero current is consistent with the Earth's magnetic field. The power supplies were current-regulated. Field measurements were made using the Walker Scientific MG-10D gaussmeter. According to the manufacturer, this meter has a resolution of 10 milligauss, an accuracy of 0.05% and is autocompensated for probe linearity and temperature.

Heat buildup was a concern so aluminum fins were buried in the coils and extended outside the coils to help radiate heat. In addition, an Omega CN101 high temperature alarm, with six thermocouples buried in the coils, was used to monitor the coil temperature and trip off the power supplies if the coil temperature exceeded 70^{o}C. Figure 3 shows shows the average temperature of the six thermocouples at maximum current as a function of time. The error bars represent the spread of temperatures among the six thermocouples. The coils were powered for about 10 minutes after which one of the thermocouples registered 70^{o}C, turning off the supply. The exponential cooldown had a time constant of about 100 min.

2.2 Field measurements and calculations

The magnetic field within the space between the Helmholtz coils was determined using TOSCA, a finite-element software package to solve three-dimensional magnetostatics equations. Figure 4 shows a comparison of the TOSCA simulation of the field, given the geometry of the current distribution, with field measurements. The magnetic field was also calculated using *Mathematica* taking into account the finite distribution of currents. Figure 5 shows a schematic of the coils. The darkened volume shown is defined by the requirement that the field throughout the volume deviates from the central field by no more than 10%.

3 Shielding studies

3.1 Effects of shielding with iron and μ-metal

Initial shielding measurements were made using a cylinder of MT1010 annealed iron with a length of 9.5 in, an outer diameter of 3.13 in. and a wall thickness of 0.063 in. Measurements were made as a function of position inside and outside of the iron alone and with the addition of co-netic μ-metal shielding. The measurements were made at a current corresponding to a central field of 82 G with no iron present. Figure 6 shows the comparison of measurements with TOSCA for simulations for the iron shielding alone. Figure 7 show the measurements and simulations for iron shielding along with μ-metal. For these measurements the axis of the cylinder was aligned along the axis of the coils. In both Figure 6 and Figure 7 the measured field along the axis at the ends of the iron cylinder is larger that the central field with no iron present. The field measurements inside the shield as shown in Figure 6 fall below the predictions fromTOSCA simulations. We note that the TOSCA simulations include the $B - H$ curves for both MT1010 iron and co-netic μ-metal shielding. For these measurements and for all other measurements with the iron shields, the shields were de-gaussed before measurements to avoid any hysteresis effects.

3.2 Effects of shield wall thickness and annealing

In order to study the shielding effectiveness as a function of wall thickness and whether or not the iron was annealed, six annealed iron shields of varying wall thicknesses and outer diameter were prepared. Another set of six shields of identical dimensions were prepared using unannealed iron. The shields were

9.0 in. long. In order to avoid confusion in making measurements the shields were color coded. The shield dimensions are summarized in Table 1. The plot of Figure 8 shows the measured magnetic field in the center of MT1010 annealed iron 9.0 in. long cylinders of varying outer diameters and wall thickness as a function of the current in the Helmholtz coils. The value of the central field at a given current is the field with no iron present. The shield with a wall thickness of 0.178 in. reduces a 180 G external field to 4 G inside the shield. From these data the conclusion is the the effectiveness of shielding increases as the total mass of the iron. The shielding of the unannealed set of iron shields was also measured. In Figure 9 we compare the shielding effect of annealed and nonannealed shields as a function of wall thickness. For the shield with a wall thickness of 0.178 in. the field inside the nonannealed shield is more than twice that of the annealed shield.

3.3 Measurements with a radioactive source

Figure 10 shows count rates measured for alpha particles from a ^{241}Am source mounted on a scintillator block attached to a FEU-84-3 phototube. The count rate (in arbitrary units) is shown as a function of central field for the thickest and thinnest iron shields under study for the longitudinal orientation where the shield/phototube are aligned along the axis of the Helmholtz coils. For the iron shield with the thinner wall (gray shield with a wall thickness of 0.066 in) the count rate starts to drop for a central magnetic field of just over 100 G in the longitudinal orientation of the phototube. For the shield with the larger wall thickness (green shield with a wall thickness of 0.178 in) the count rate for the longitudinal orientation does not decrease appreciably until the central field reaches 180 G. In the transverse orientation the shield/phototubes are aligned perpendicular to the axis of the coils. For the transverse orientation of the phototubes, the count rate (not shown) remains constant with increasing central magnetic field for both the thinner and thicker shields. In all cases the μ-metal shielding was used in addition to the iron.

3.4 Photocathode position in the shield

We examined the effect of shielding as a function of distance of the phototube photocathode from the end of the shield. A tube/shield assembly consisting of a Philips XP2020 and an iron shield with an outer diameter of 2.75 in, an inner diameter of 2.48 in. and a length of 17 in. was used. The XP2020 has an outer diameter of 2.4 in and a nominal photocathode diameter of 2 in. The assembly was oriented perpendicular to the central field of the Helmholtz coils and the distance from the photocathode to the end of the shield was varied.

The measured magnetic field outside the edge of the shield was 100 G. The rate from the ^{241}Am/scintillator source described previously was measured for various locations of the photocathode relative to the end of the magnetic shield. Figure 11 shows the rate as a function of position. The usual prescription that the photocathode must be placed one tube diameter inside the shield is supported by these measurements.

4 Summary

The construction and operation of a Helmholtz coil arrangement to produce a magnetic field of up to 200 G is presented. Even at the the maximum current the coils can be operated for periods of about 10 min but it is essential to employ a temperature trip mechanism. Measurement of the magnetic field inside various iron and μ-metal shields are well described using TOSCA simulations. From our studies we conclude that iron shields and μ-metal will provide adequate shielding of phototubes for the TOF and FCAL in the fringe field of the GlueX superconducting magnet.

Acknowledgements

We want to thank Paul Brindza for his guidance on the use of TOSCA and general advice on dealing with the fringe field of the superconducting solenoid. We also thank members of the GlueX collaboration. We acknowledge financial support from the US Department of Energy and the Russian Fund for Basic Researches (grants 1305.2003.2 and 02-02-17019). The Southeastern Universities Research Association (SURA) operates the Thomas Jefferson National Accelerator Facility for the U.S. Department of Energy under contract DE-AC05-84ER40150.

References

[1] GlueX Design Report available at `www.gluex.org`. See also A. Dzierba, Int. Jour. Mod. Phys., **A18** (2003) 397.

[2] S. Denisov *et. al.*, Nucl.Instr. and Meth., **A494** (2002) 495.

[3] B. Brabson *et. al.*, Nucl.Instr. and Meth., **A332** (1993) 419.

[4] R. Crittenden *et. al.*, Nucl.Instr. and Meth., **A387** (1997) 377.

Table 1
Color coded iron shields with outer diameter and thickness dimensions.

Color code	Outer Diameter (in.)	Thickness (in.)
Gray	2.746	0.066
Yellow	2.507	0.083
Black	2.499	0.115
Red	2.997	0.120
Blue	2.745	0.122
Green	3.000	0.178

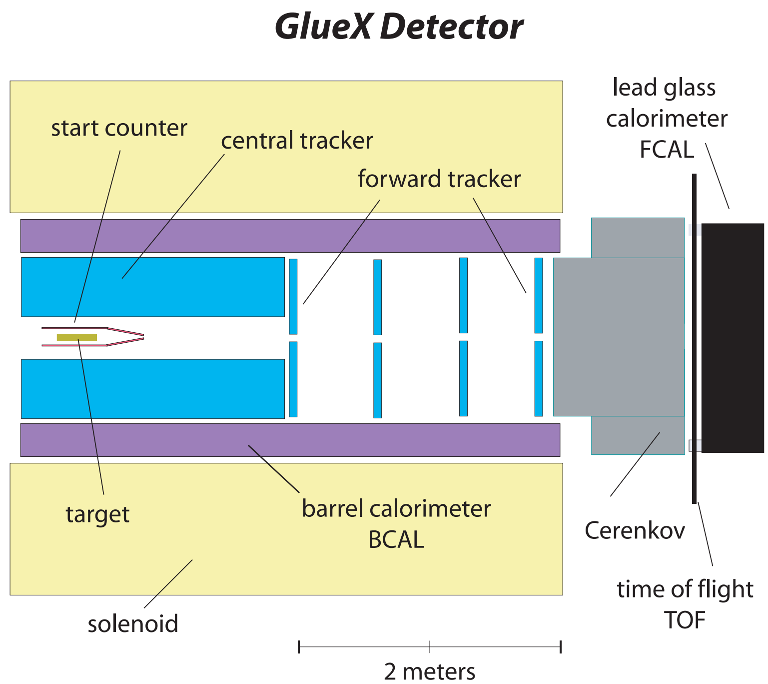

Fig. 1. Schematic of the GlueX detector.

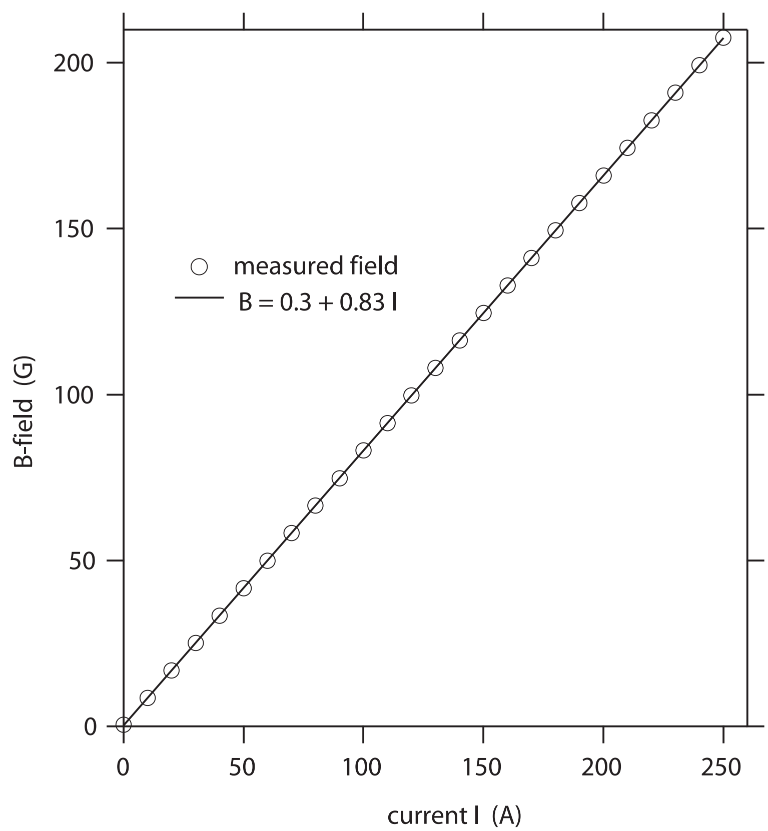

Fig. 2. Central B-field as a function of the total power supply current.

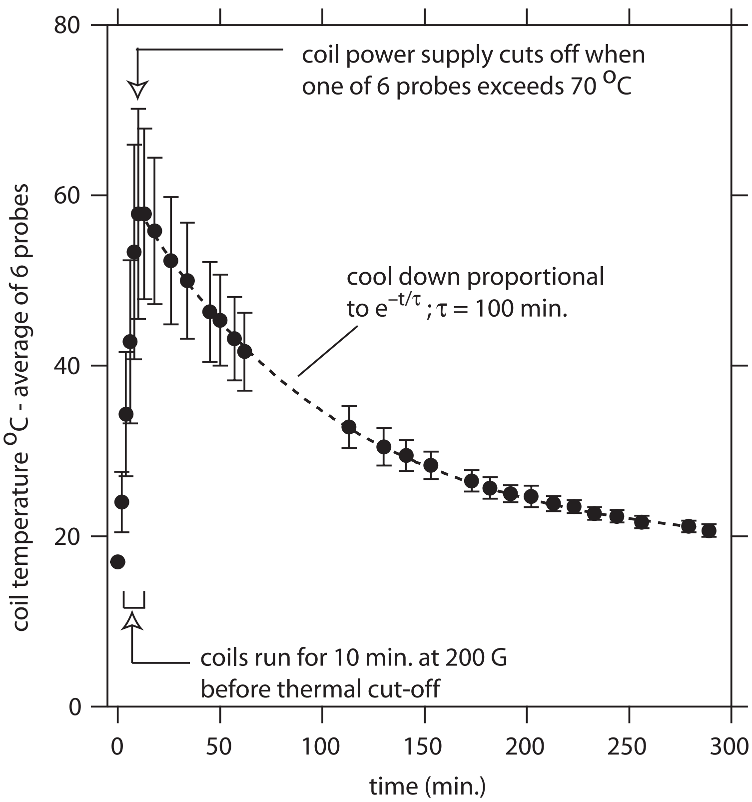

Fig. 3. Temperature of the Helmholtz coils as a function of time. Details are given in the text.

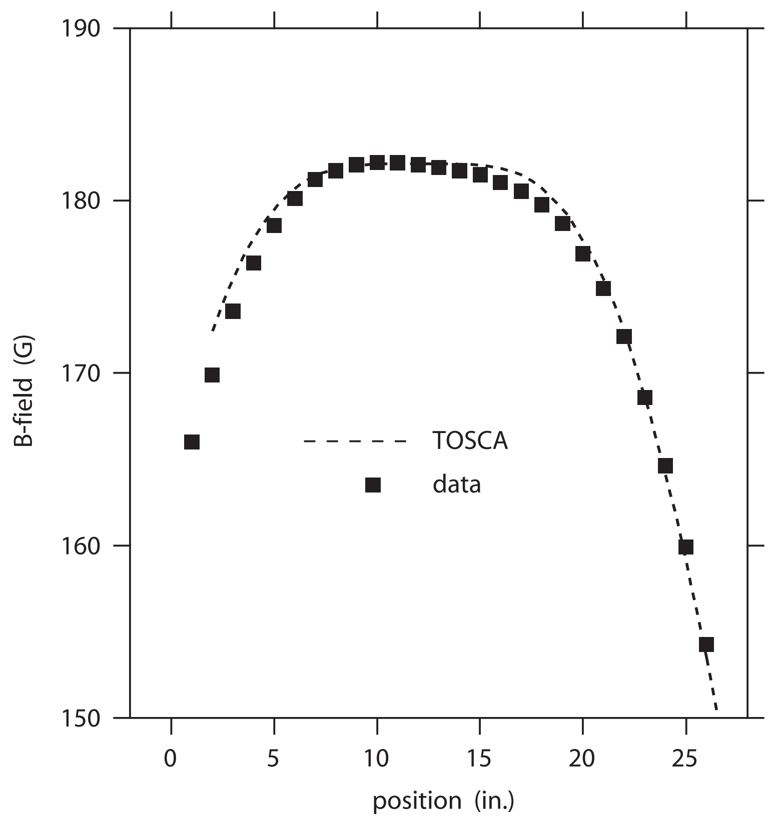

Fig. 4. A comparison of the TOSCA simulation of the magnetic field of the Helmholtz coils with measurements. The coil separation is approximately 50 cm or 20 in.

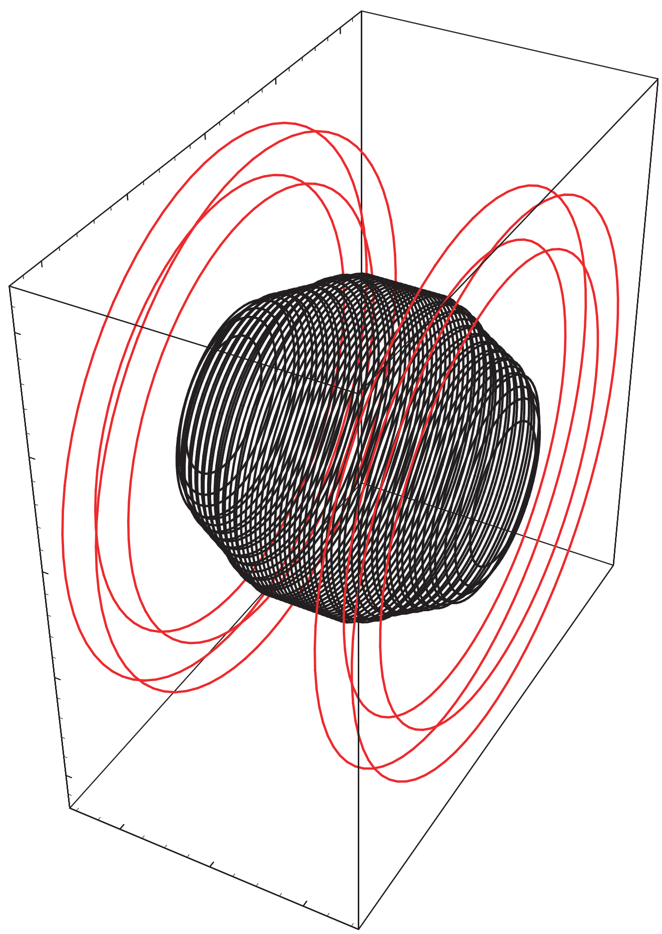

Fig. 5. A schematic of the Helmholtz coils used to perform magnetic shield studies. The coil diameter is 1.0 m and the separation 0.5 m. The darkened volume shown is defined by the requirement that the field throughout the volume deviates from the central field by no more than 10%.

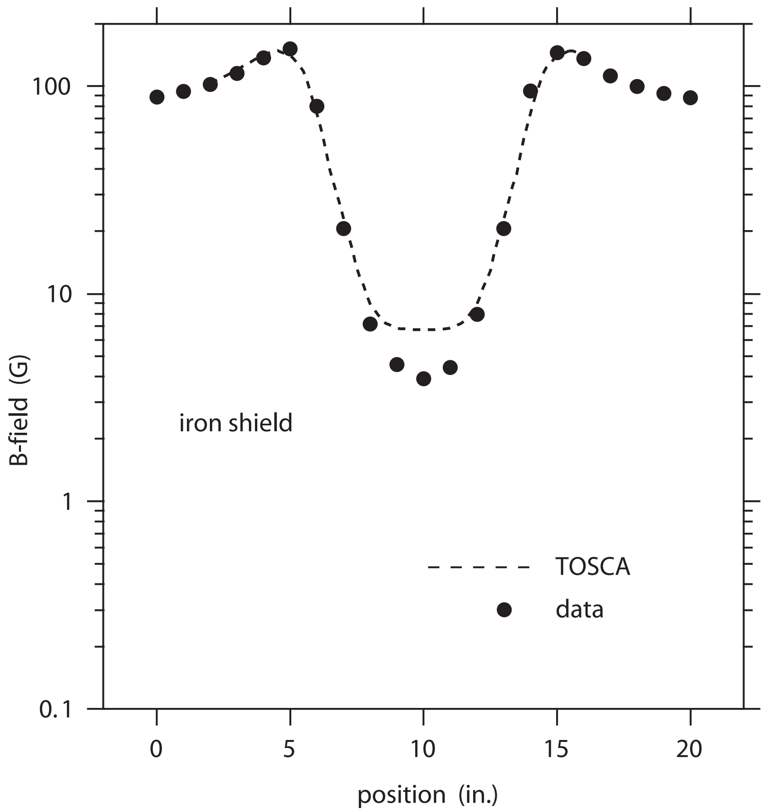

Fig. 6. A comparison of the TOSCA simulation of the magnetic field with measurements of the magnetic field along the axis of the Helmholtz coils with a 9.5 in. long iron cylinder centered between the coils and aligned with the axis of the coils. Other cylinder dimensions are given in the text. The current in the coils corresponded to a central magnetic field, without iron, of 82 G.

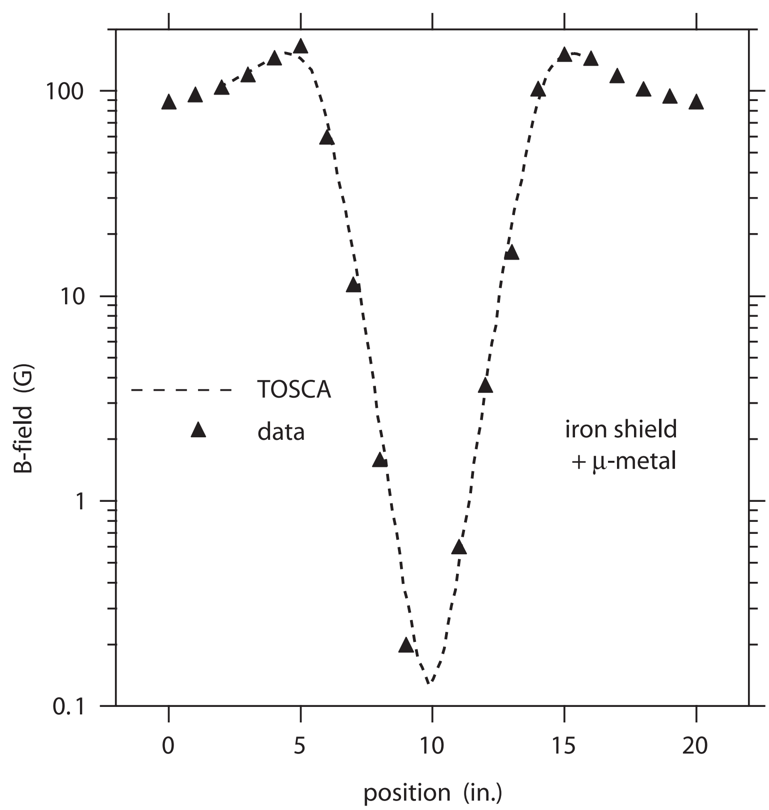

Fig. 7. Same as for Figure 6 but with the addition of co-netic μ-metal shielding inside the iron cylinder.

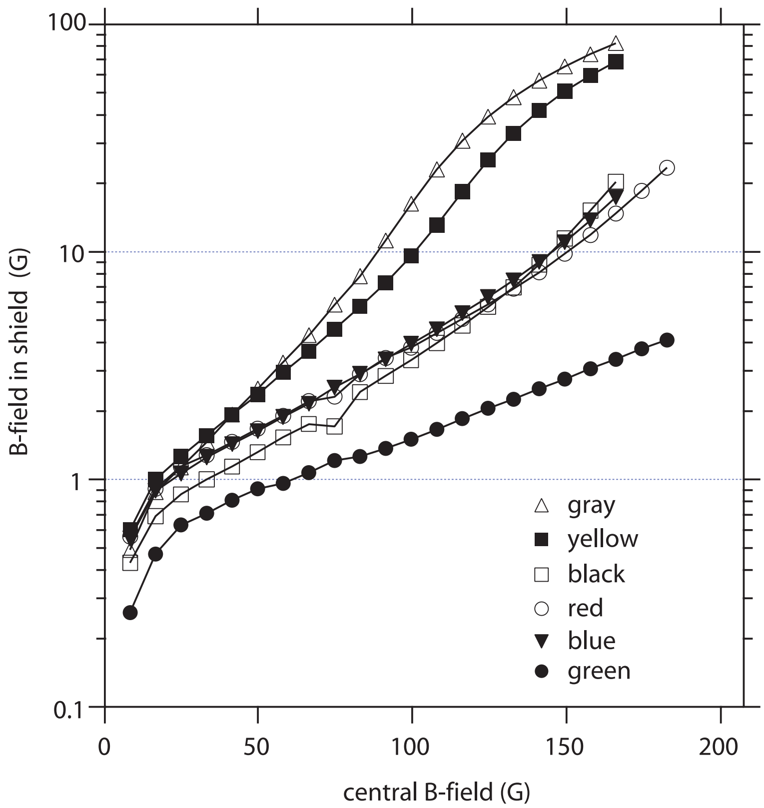

Fig. 8. The measured magnetic field in the center of 1010 annealed iron 9 in. long cylinders of varying outer diameters and wall thickness. See the text for details.

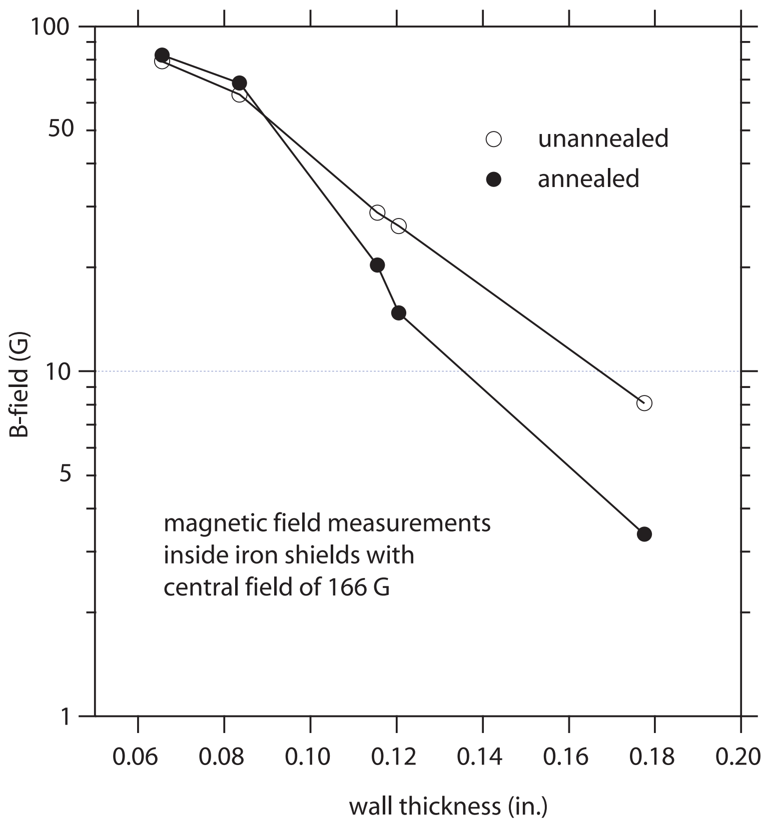

Fig. 9. The measured magnetic field in the center of iron cylindrical shield listed in Table 1 as a function of wall thickness comparing annealed iron with nonannealed iron.

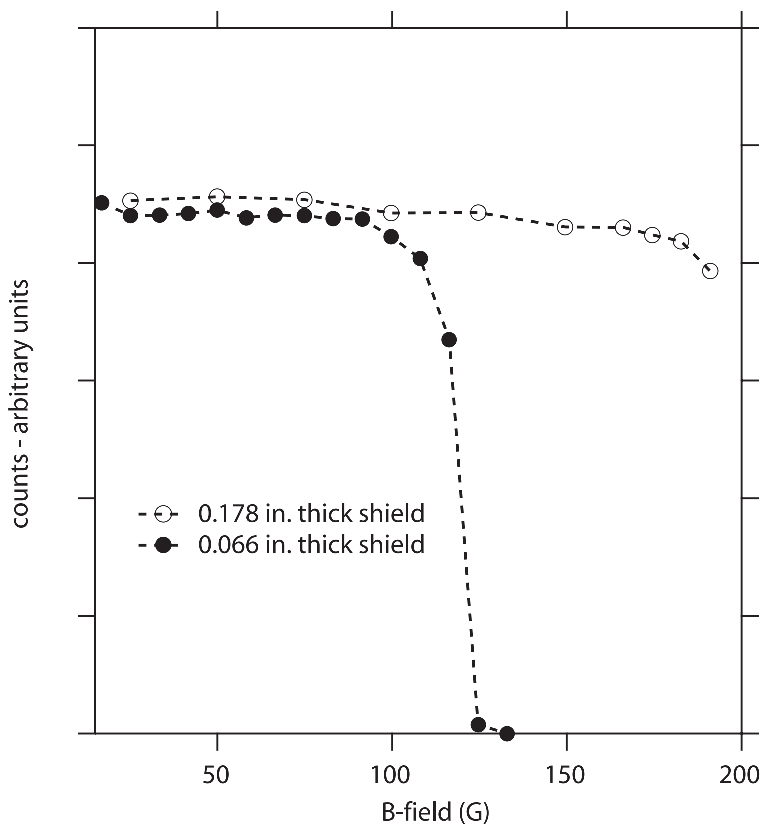

Fig. 10. Rates measured for alpha particles from a ^{241}Am source mounted on a scintillator block attached to a FEU-84-3 phototube. See the text for details.

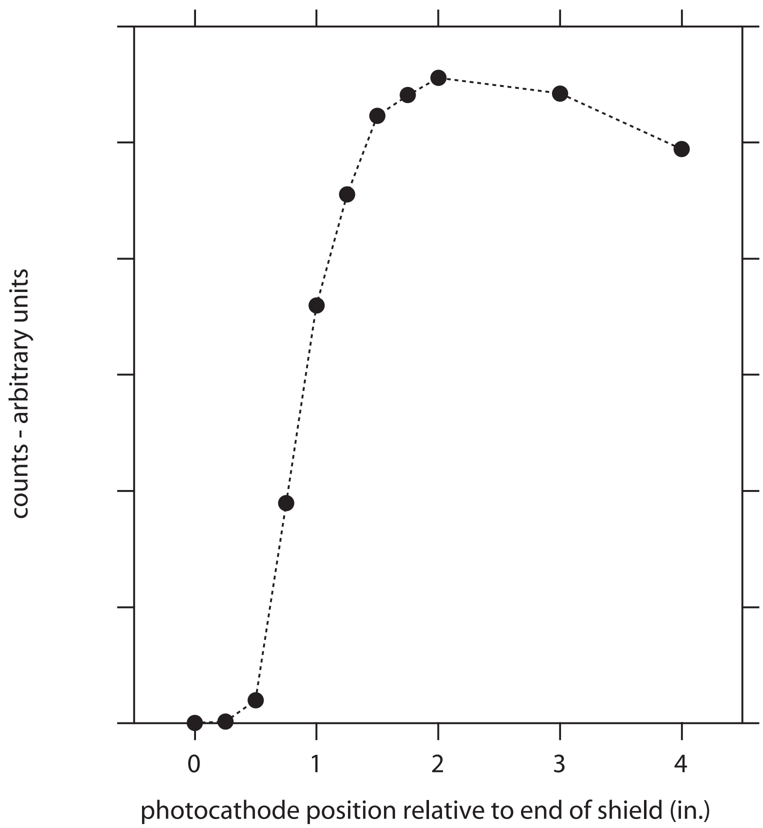

Fig. 11. Rates measured for alpha particles from a ^{241}Am source mounted on a scintillator block attached to a XP2020 phototube. The phototube was placed in an iron shield oriented perpendicular to the axis of the Helmholtz coils. The field at the edge of the shield was measured to be 100 G. The distance from the edge of the shield to the photocathode was varied. See the text for details.